*CORRESPONDENCE
Ying Shen
✉ rjshenying@qq.com
Yongning Shang
✉ ynshang@aliyun.com
Yang Dai
✉ yutongwushe@163.com

†These authors have contributed equally to this
work

Dynamic evolution of left ventricular strain and microvascular perfusion assessed by speckle tracking echocardiography and myocardial contrast echocardiography in diabetic rats: Effect of dapagliflozin

Juan Liu[1†], Yixuan Wang[2†], Jun Zhang[1], Xin Li[1], Lin Tan[1], Haiyun Huang[1], Yang Dai[2]*, Yongning Shang[1]* and Ying Shen[2]*

[1]Department of Ultrasound, Southwest Hospital, Army Medical University (Third Military Medical University), Chongqing, China, [2]Department of Cardiovascular Medicine, Rui Jin Hospital, Shanghai Jiaotong University School of Medicine, Shanghai, China

Background: This experimental study aimed to determine the dynamic changes in myocardial strain and microvascular perfusion in diabetic rats by comprehensive echocardiography while evaluating the effect of dapagliflozin (DAPA).

Materials and methods: Male Sprague−Dawley rats ($n = 128$) were randomly divided into four groups based on the presence or absence of a high-fat diet and streptozotocin-induced diabetes with or without DAPA treatment ($n = 32$/group). Serial conventional ultrasound, two-dimensional speckle tracking echocardiography (2D-STE) and myocardial contrast echocardiography (MCE) were performed at 2, 4, 6, and 8 weeks, and left ventricular global longitudinal strain (GLS), myocardial blood flow velocity (MBFV), myocardial blood flow (MBF), and myocardial blood volume (MBV) were determined. All animals were sacrificed immediately after the last echo measurement for histopathological assessment.

Results: Despite similar conventional Doppler-echo indexes among the groups at 2, 4, 6, and 8 weeks ($p > 0.05$), left ventricular GLS, MBFV, MBF, and MBV were decreased at 8 weeks in diabetic rats ($p < 0.05$) as detected by both 2D-STE and MCE. These indexes were significantly improved at 6 and 8 weeks after treatment with DAPA for diabetic rats ($p < 0.05$), reaching similar values observed in non-diabetic controls. DAPA treatment was associated with increased myocardial vacuolization and microvessel density and reduced interstitial fibrosis in diabetic rats.

Conclusions: Combined 2D-STE and MCE is sensitive for detecting left ventricular deformity and impaired microvascular perfusion in prediabetes and the early stage

of diabetes mellitus. DAPA exerts a beneficial effect on protecting myocardial perfusion in diabetic rats.

1. Introduction

It is well recognized that chronic hyperglycemia reduces the self-protective ability of vascular endothelial cells, impairs microvascular perfusion, and decreases cardiac systolic and diastolic function, ultimately leading to diabetic cardiomyopathy. Cardiac dysfunction in the absence of coronary artery disease, hypertension, and valvular disease is called diabetic cardiomyopathy, which is one of the most common complications of diabetes mellitus (DM). The main pathological changes of diabetic cardiomyopathy includes myocardial interstitial fibrosis, myocardial stiffness and microvascular rarefaction, eventually leading to diastolic and systolic dysfunction. Timely intervention of diabetic cardiomyopathy is very challenging (1), therefore, the detection of alterations in myocardial and microvascular function in the process from prediabetes to the early stage of diabetes mellitus (earlyDM) plays a vital role in the prevention of serious complications (2). Although conventional ultrasound techniques, such as M-mode, two-dimensional echocardiography, coupled with color Doppler flow and tissue Doppler imaging, are routinely used for evaluating cardiac structure and function, two-dimensional speckle tracking echocardiography (2D-STE) provides quantitative assessment of local and global left ventricular mechanical changes (3), and myocardial contrast echocardiography (MCE) serves as a tool to determine the total amount and speed of myocardial microvascular blood perfusion (4). However, data are lacking concerning the role of these techniques used alone or in combination for evaluating dynamic changes in myocardial function and microvascular perfusion, especially for patients with diabetes mellitus.

Several randomized trials and observational studies have shown that sodium-glucose cotransporter 2 (SGLT2) inhibitors significantly reduce the risk of cardiovascular adverse events in diabetic patients (5–7). Further studies indicated that these agents could also provide beneficial cardiovascular effects even for non-diabetic patients, suggesting that myocardial protection with SGLT2 inhibitors may occur through a glucose-independent pathway (8–10). Nevertheless, further in-depth studies are warranted to clarify the mechanism of the protective effect of SGLT2 inhibitors on the myocardium.

Since changes in myocardial function and microvascular perfusion in prediabetes and earlyDM have not yet been well studied and whether early intervention with SGLT2 inhibitors can effectively prevent myocardial damage is not clear, in this experimental study, we used conventional ultrasound techniques, 2D-STE and MCE, to evaluate the dynamic evolution of myocardial function and microvascular perfusion and to explore the potential beneficial effect of the SGLT2 inhibitor dapagliflozin (DAPA) in a diabetic rat model.

2. Materials and methods
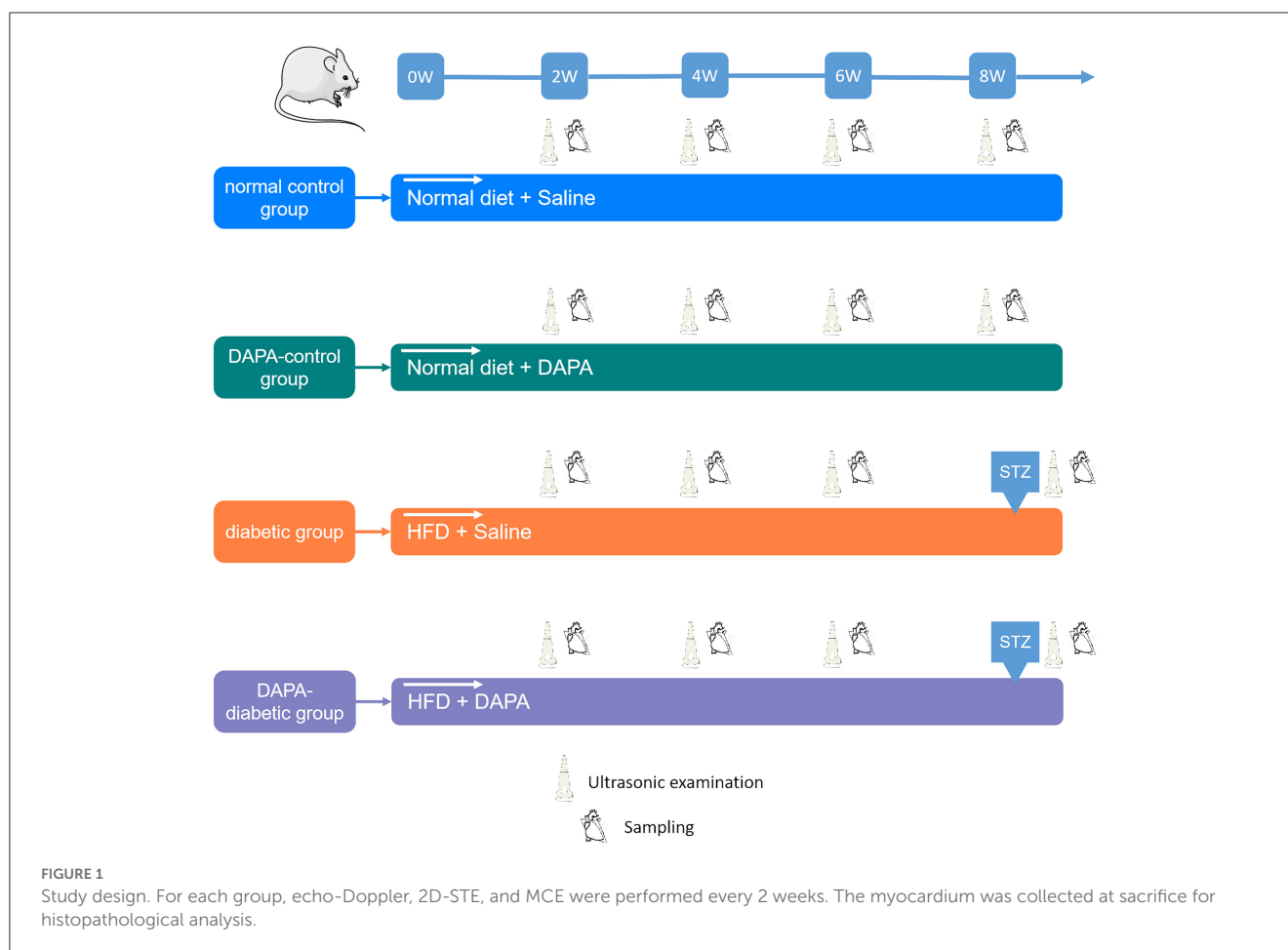
2.1. Animal model and groups

Male Sprague–Dawley rats (120–150 g) aged 5 weeks were obtained from the Laboratory Animal Center of the Third Military Medical University and kept in a constant temperature and humidity environment under a 12-h light/dark cycle with free access to food and water. The experimental protocol was approved by the Laboratory Animal Welfare and Ethics Committee of the Third Military Medical University (No. AMUWEC20224071).

A total of 128 animals were randomly divided into four groups ($n = 32$ in each group): the normal control group included rats with 8 weeks of standard diet plus saline followed by citrate buffer; the DAPA-control group consisted of rats with 8 weeks of standard diet plus oral administration of DAPA followed by citrate buffer; the diabetic group comprised rats with 8 weeks of high-fat diet (HFD) plus saline followed by intraperitoneal injection of streptozotocin (STZ), and the DAPA-diabetic group comprised rats with 8 weeks of HFD plus oral administration of DAPA followed by intraperitoneal injection of STZ. In brief, a HFD consists of 79.85% general animal feed, 15% fat (oil), 5% custard powder, and 0.15% cholesterol (Laboratory Animal Center of the Third Military Medical University). DAPA (AstraZeneca) was given orally at a dose of 1 mg/kg/d for 8 weeks. STZ (Sigma–Aldrich, St. Louis, MO) was injected at a dose of 30 mg/kg under fasting conditions, and diabetes was identified when the fasting blood glucose level was >11.1 mmol/L at day 5 (Figure 1).

2.2. Conventional Doppler echocardiography

Ultrasound scanning of rats was performed under anesthesia with 3% isoflurane and oxygen with a heart rate maintained at 300∼400 beats/min. Animals were placed on a prewarmed rodent platform, and body temperature was maintained at approximately 37°C. The anterior chest hair was then cleared.

An ultrahigh resolution animal imaging system (VEVO 2100, VisualSonics, Toronto, Canada) with a linear array probe (MS400, a frequency of 24 MHz) was used to carry out conventional transthoracic echocardiography. M-mode images were recorded at the level of the papillary muscles in the best parasternal long

FIGURE 1
Study design. For each group, echo-Doppler, 2D-STE, and MCE were performed every 2 weeks. The myocardium was collected at sacrifice for histopathological analysis.

axis view. Left ventricular end-diastolic (EDD) and end-systolic diameters (ESD) and end-diastolic posterior wall thickness (PWd) and interventricular septum thickness in diastole (IVSd) were measured, and fractional shortening (FS) and left ventricular mass index (LVMI) were calculated. Left ventricular end-diastolic (EDV) and end-systolic volumes (ESV) and ejection fraction (EF) were determined by two-dimensional echocardiography. An average of three consecutive cycles was used.

Spectral Doppler in the best 4-chamber view with the sampling site positioned at the level of the mitral valve was used to measure peak flow velocity (E), isovolumic systolic time (ICT), isovolumic diastolic time (IRT), and LV ejection time (ET). Tissue Doppler imaging (TDI) was applied to determine myocardial motion velocity (e') at the junction between the septum and mitral annulus. The ratio of E to e' (E/e') and the Tei index, (ICT + IRT)/ET, were calculated (11).

2.3. Two-dimensional speckle tracking echocardiography

Parasternal long- and short-axis images were acquired for at least 3 cardiac cycles with optimal visualization of the LV myocardium. 2D-STE analysis was performed offline using TOMTEC software (TOMTEC Image System GmbH,

Germany). Both endocardial and epicardial boundaries of the left ventricular myocardium were manually traced. This software can automatically track the movement of the entire myocardium. All tracked contours were checked, and, when poorly tracked, the data were excluded. Left ventricular global longitudinal strain (GLS), global circumferential strain (GCS), and global radial strain (GRS) were then derived. All values were averaged from 3 cardiac cycles.

2.4. Myocardial contrast echocardiography

Real-time MCE was performed using a Philips ultrasound diagnostic system (EPIC 7, Philips Medical Systems, Andover, MA, USA) with a linear array probe (eL18-4, 20 MHz). In brief, a commercially available contrast agent (SonoVue, Bracco, Italy) was diluted twice by adding 5 ml of normal saline, and a 24-gauge cannula was placed into the tail vein with continuous infusion (0.3–0.4 ml/min) (12). All images were optimized for each animal, including penetration depth 2 cm, near field focused on the middle of the left ventricle, gains adjusted without signal intensity of the myocardium, maximal dynamic range (60 dB), and mechanical index 0.06. When contrast agent was filled in the myocardium, left ventricular parasternal long axis images were stored for at least 20 cardiac cycles. The "flash (high energy pulse, mechanical index >1.0)" function was

TABLE 1 Conventional echo-Doppler measurements.

	Normal control				DAPA-control				Diabetic				DAPA-diabetic			
	2W (n = 8)	4W (n = 8)	6W (n = 8)	8W (n = 8)	2W (n = 8)	4W (n = 8)	6W (n = 8)	8W (n = 8)	2W (n = 8)	4W (n = 8)	6W (n = 8)	8W (n = 8)	2W (n = 8)	4W (n = 8)	6W (n = 8)	8W (n = 8)
IVSd (mm)	1.81 ± 0.21	1.80 ± 0.21	1.77 ± 0.09	1.91 ± 0.13	1.75 ± 0.15	1.82 ± 0.14	1.85 ± 0.13	1.86 ± 0.10	1.78 ± 0.20	1.81 ± 0.12	1.87 ± 0.12	1.97 ± 0.17	1.84 ± 0.12	1.79 ± 0.16	1.82 ± 0.14	1.89 ± 0.12
EDD (mm)	6.92 ± 0.25	7.05 ± 0.32	7.20 ± 0.17	7.19 ± 0.26	6.88 ± 0.46	7.13 ± 0.25	7.17 ± 0.14	7.24 ± 0.32	6.82 ± 0.37	7.20 ± 0.28	7.02 ± 0.44	6.98 ± 0.26	6.82 ± 0.38	7.05 ± 0.39	7.28 ± 0.32	7.24 ± 0.49
ESD (mm)	3.09 ± 0.44	3.13 ± 0.42	3.38 ± 0.27	3.43 ± 0.19	3.21 ± 0.17	3.36 ± 0.21	3.36 ± 0.17	3.45 ± 0.17	3.18 ± 0.32	3.39 ± 0.18	3.43 ± 0.33	3.55 ± 0.20	3.33 ± 0.24	3.36 ± 0.18	3.41 ± 0.21	3.47 ± 0.18
PWd (mm)	1.86 ± 0.14	1.81 ± 0.24	1.88 ± 0.15	1.92 ± 0.09	1.80 ± 0.20	1.81 ± 0.17	1.87 ± 0.07	1.96 ± 0.10	1.88 ± 0.19	1.86 ± 0.12	1.94 ± 0.22	1.98 ± 0.16	1.82 ± 0.17	1.87 ± 0.15	1.87 ± 0.20	1.83 ± 0.16
EF (%)	83.07 ± 3.49	82.62 ± 3.41	82.69 ± 3.03	82.11 ± 2.17	82.19 ± 1.77	82.51 ± 2.75	82.85 ± 1.77	82.16 ± 1.64	82.52 ± 2.51	82.55 ± 2.72	81.16 ± 2.53	79.30 ± 2.83	82.34 ± 3.21	81.93 ± 3.13	82.89 ± 1.63	82.35 ± 2.84
FS (%)	53.36 ± 4.17	52.97 ± 3.89	53.05 ± 3.34	52.34 ± 2.48	52.23 ± 1.98	52.79 ± 3.01	53.13 ± 1.99	52.38 ± 1.85	52.75 ± 2.80	52.86 ± 3.06	51.23 ± 2.74	49.42 ± 2.64	51.13 ± 3.69	52.13 ± 3.47	53.21 ± 1.81	52.52 ± 3.40
LVMI (mg/g)	3.29 ± 0.41	2.10 ± 0.28	1.82 ± 0.22	1.76 ± 0.22	3.35 ± 0.59	2.09 ± 0.18	1.88 ± 0.34	1.90 ± 0.31	3.24 ± 0.21	1.77 ± 0.17	1.57 ± 0.13	1.49 ± 0.31	3.39 ± 0.50	1.83 ± 0.27	1.73 ± 0.14	1.67 ± 0.31
EDV (uL)	244.87 ± 33.99	268.12 ± 26.33	272.58 ± 14.77	271.85 ± 22.31	242.85 ± 32.43	266.79 ± 20.94	269.60 ± 47.01	276.35 ± 28.57	241.50 ± 29.57	272.28 ± 23.80	262.77 ± 40.61	254.48 ± 21.85	241.79 ± 30.78	260.05 ± 32.02	276.98 ± 31.43	279.21 ± 36.88
ESV (uL)	40.05 ± 10.63	46.37 ± 8.77	47.29 ± 9.43	48.55 ± 6.42	43.22 ± 4.02	46.50 ± 6.97	46.27 ± 5.48	49.21 ± 5.94	40.81 ± 10.10	47.20 ± 6.08	48.94 ± 10.69	52.78 ± 7.35	43.10 ± 4.72	46.44 ± 5.92	47.88 ± 7.17	50.02 ± 6.47
E/e'	14.13 ± 0.83	14.09 ± 0.86	13.99 ± 1.28	14.02 ± 1.82	13.95 ± 1.42	14.04 ± 0.84	14.21 ± 0.96	14.07 ± 1.06	14.01 ± 1.01	14.15 ± 1.23	14.50 ± 1.50	15.01 ± 1.11	14.15 ± 1.09	14.02 ± 1.45	14.06 ± 1.09	14.12 ± 1.39
Tei index	0.49 ± 0.07	0.50 ± 0.09	0.50 ± 0.14	0.50 ± 0.11	0.49 ± 0.06	0.49 ± 0.11	0.52 ± 0.07	0.53 ± 0.08	0.48 ± 0.11	0.52 ± 0.11	0.53 ± 0.10	0.56 ± 0.13	0.51 ± 0.06	0.50 ± 0.11	0.51 ± 0.06	0.53 ± 0.08

IVSd, interventricular septum thickness in diastole; EDD, Left ventricular end-diastolic diameter; ESD, Left ventricular end-systolic diameter; PWd, Left ventricular end-diastolic posterior wall thickness; EF, ejection fraction; FS, fractional shortening; LVM, Left ventricular mass; LVMI, Left ventricular mass index; EDV, Left ventricular end-diastolic volume; ESV, Left ventricular end-systolic volume; E, peak flow velocity; e', myocardial motion velocity.

FIGURE 2
Comparison of conventional echo-Doppler data among groups. **(A)** EF, E/e', and Tei of the four groups at different time points. **(B)** Differences in EF, E/e', and Tei among the four groups at different time points. **(C)** Representative M-mode images, spectral Doppler images, and tissue Doppler images of the four groups at 8 weeks. (1) normal control group, (2) DAPA-control group, (3) diabetic group, (4) DAPA-diabetic group. EF, ejection fraction; E, peak flow velocity; e', myocardial motion velocity; Tei, Tei index; NC, normal control group; DAPA-C, DAPA-control group; DM, diabetic group; DAPA-DM, DAPA-diabetic group.

immediately triggered to destroy all myocardial microbubbles and then automatically switched to a low-energy real-time contrast state.

All video recordings were analyzed offline using a QLAB (version 6.0, Philips Healthcare) workstation. Regions of interest (ROIs) were manually placed on the middle segment of the anterior myocardium with an area of approximately 1.5 mm^2, and each frame was manually checked to avoid partial volume effects from the right and left ventricular cavities. The first frame image after "flash" was set as the background frame, and then the time-signal intensity curve was fitted to an exponential function (13):

$$Y = A\left(1 - e^{-\beta t}\right) + C,$$

where A is the peak intensity in the plateau phase, reflecting myocardial blood volume (MBV), β is the rising slope of signal intensity, reflecting myocardial blood flow velocity (MBFV), and A*β equals myocardial blood flow (MBF) (14).

2.5. Histopathological examination

After MCE, all animals were anesthetized in an unconscious state, then euthanized with thoracotomy and heart removal. The heart was fixed in 4% neutral buffered formalin and embedded in paraffin, then serially sectioned along the long axis of the left ventricular papillary muscle (4 μm thick), which was similar to the MCE plane. Hematoxylin and eosin (H&E) staining was performed to assess cardiac histomorphological changes. Masson's trichrome staining was performed to visualize the status of cardiac tissue fibrosis, and CD31 (Abcam ab182981) was used to evaluate myocardial vessels, which were subsequently examined by a pathologist who was blinded to the ultrasonic results.

2.6. Statistical analysis

The Shapiro–Wilk test was performed to evaluate the distribution of the data. Continuous and normally distributed data were presented as mean ± SD. Differences among groups were determined by one-way ANOVA followed by Bonferroni *post hoc*

TABLE 2 Left ventricular strain data by 2D-STE.

		Normal control ($n = 32$)	DAPA-control ($n = 32$)	Diabetic ($n = 32$)	DAPA-diabetic ($n = 32$)
2W	GLS (%)	-21.78 ± 2.13	-20.04 ± 3.21	-20.95 ± 3.14	-20.34 ± 3.52
	GCS (%)	-20.23 ± 2.31	-20.92 ± 3.05	-21.59 ± 3.21	-20.26 ± 3.86
	GRS (%)	47.82 ± 2.55	46.95 ± 6.58	48.41 ± 5.53	46.49 ± 4.53
4W	GLS (%)	-21.31 ± 2.18	-19.13 ± 3.66	-19.08 ± 2.75	-19.75 ± 3.02
	GCS (%)	-21.68 ± 2.66	-21.10 ± 2.29	-21.09 ± 2.63	-21.80 ± 4.62
	GRS (%)	48.01 ± 3.15	46.71 ± 5.20	46.21 ± 6.10	47.24 ± 3.82
6W	GLS (%)	-20.93 ± 3.12	-19.03 ± 2.24	-18.98 ± 3.35	-18.45 ± 3.68
	GCS (%)	-20.19 ± 2.97	-19.62 ± 2.03	-19.14 ± 2.35	-19.88 ± 3.43
	GRS (%)	48.41 ± 4.81	47.76 ± 4.91	45.12 ± 5.24	46.81 ± 5.83
8W	GLS (%)	-21.02 ± 2.96	-20.42 ± 3.43	-16.24 ± 2.42[*#†]	-19.09 ± 2.06
	GCS (%)	-20.58 ± 4.07	-19.44 ± 3.62	-18.24 ± 2.23	-19.18 ± 2.49
	GRS (%)	46.83 ± 3.75	46.55 ± 5.71	43.55 ± 4.52	46.14 ± 5.25

GLS, global peak longitudinal strain; GRS, global peak radial strain; GCS, global peak circumferential strain. [*]$p < 0.05$ vs. normal control group; [†]$p < 0.05$ vs. DAPA-control group; [#]$p < 0.05$ vs. diabetic group at 2 weeks.

tests. A value of $p < 0.05$ was considered significant. All statistical analyses were performed by SPSS (version 21.0, SPSS Inc., Chicago, IL, USA), and GraphPad Prism (version 7.04, GraphPad Software, Inc., La Jolla, CA, USA) was used to generate statistical figures.

3. Results

3.1. Comparison of conventional echo-Doppler results

Left ventricular geometric measurements, E/e' and Tei index were unchanged among the four groups from 2 to 8 weeks (all $p > 0.05$). The left ventricular EF decreased gradually in the diabetic group but remained stable in the DAPA-diabetic group. However, the difference did not reach statistical significance (Table 1, Figure 2).

3.2. Comparison of 2D-STE data

In the diabetic group, GLS decreased stepwise from 2 to 8 weeks, with a statistically significant difference between 2 and 8 weeks ($p = 0.02$). At 8 weeks, left ventricular strain parameters were significantly reduced in the diabetic group compared to the normal control ($p = 0.011$) and DAPA-control groups ($p = 0.032$). However, no differences were observed among the normal control, DAPA-control, and DAPA-diabetic groups (Table 2, Figure 3).

3.3. Comparison of MCE quantitative data

In the diabetic group, the values of myocardial perfusion as expressed by MBFV and MBF decreased stepwise from 2 to 8 weeks, with statistically significant differences between 2 and 6 weeks ($p = 0.019$, $p = 0.023$) and 2 and 8 weeks ($p = 0.001$, $p = 0.001$).

Compared with the normal control and DAPA-control groups, MBFV, MBF, and MBV were decreased gradually in the diabetic group across 2, 4, 6, and 8 weeks, reaching levels of statistically significant differences at 6 weeks for MBFV and MBF ($p = 0.047$, $p = 0.026$) and at 8 weeks for MBV ($p = 0.033$). There were no significant differences in these values among the normal control, DAPA-control, and DAPA-diabetic groups (Table 3, Figure 4).
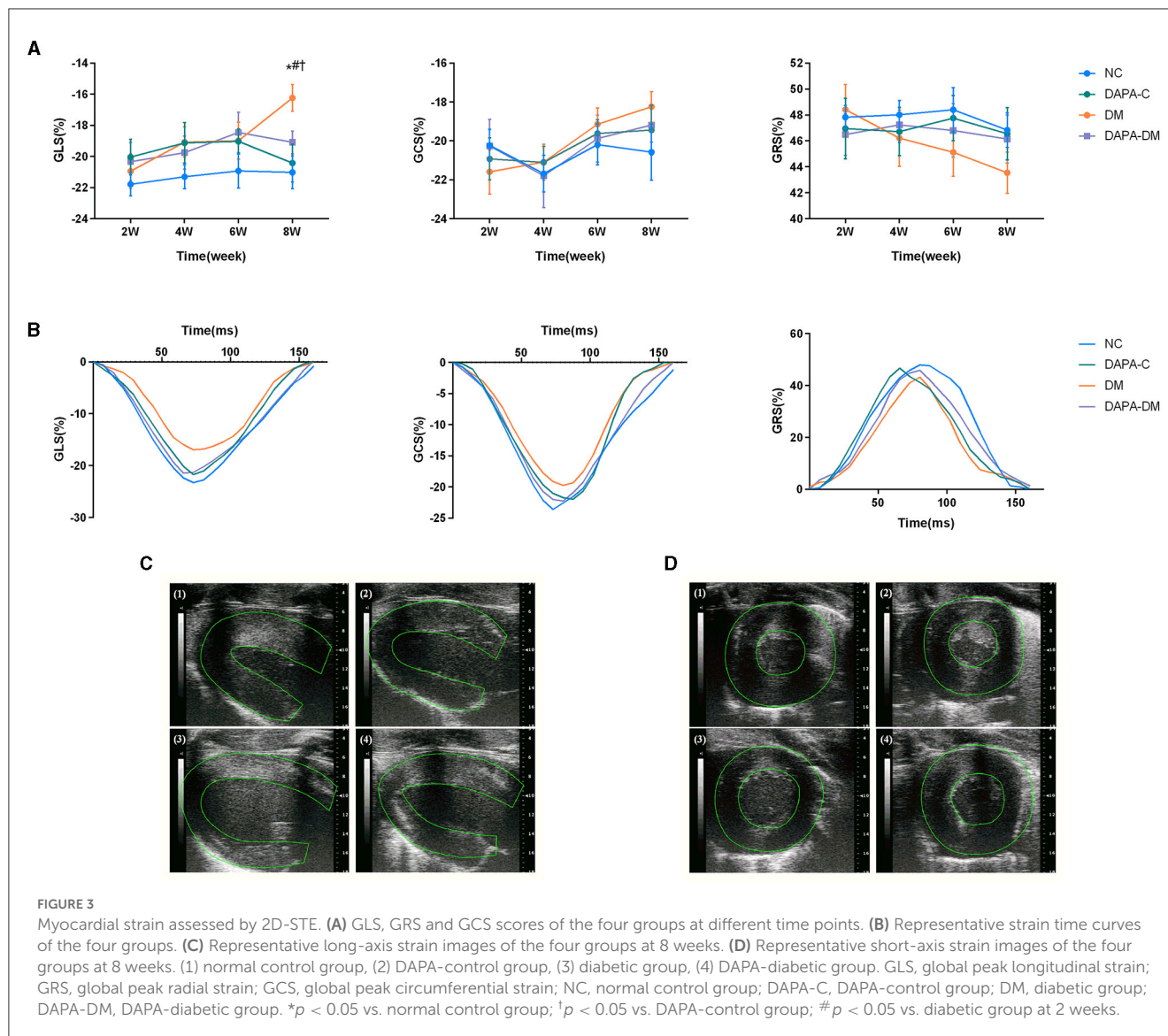
3.4. Histopathological findings

Histopathological changes were found in the diabetic group. Figure 5 shows typical tissue morphology following H&E, Masson's trichrome, and CD31 staining in each group at 8 weeks. In the normal control group, myocardial cell morphology was normal, with closely packed cells. In contrast, in the diabetic group, myocardial cells were vacuolated and disorganized; increased collagen fibers deposition and decreased myocardial microvascular density were also seen. However, in the DAPA-diabetic group, the morphology of myocardial cells was essentially normal, with closely packed cells. In addition, myocardial fibrosis and myocardial microvascular density decreased were not as obvious.

4. Discussion

The results of this study showed that the combined use of 2D-STE and MCE was a sensitive way to detect left ventricular deformity and impaired microvascular perfusion in prediabetes and earlyDM. DAPA exerts a cardio-protective effect in this setting.

Myocardial dysfunction of varying degrees often occurs in earlyDM (15). With the prolongation of the disease process, disturbance of energy metabolism causes myocardial and endothelial cell remodeling, apoptosis, fibrosis and myocardial microvascular abnormalities (16–18). In addition, increased wall thickness and mass reduce left ventricular diastolic compliance

FIGURE 3
Myocardial strain assessed by 2D-STE. **(A)** GLS, GRS and GCS scores of the four groups at different time points. **(B)** Representative strain time curves of the four groups. **(C)** Representative long-axis strain images of the four groups at 8 weeks. **(D)** Representative short-axis strain images of the four groups at 8 weeks. (1) normal control group, (2) DAPA-control group, (3) diabetic group, (4) DAPA-diabetic group. GLS, global peak longitudinal strain; GRS, global peak radial strain; GCS, global peak circumferential strain; NC, normal control group; DAPA-C, DAPA-control group; DM, diabetic group; DAPA-DM, DAPA-diabetic group. *$p < 0.05$ vs. normal control group; †$p < 0.05$ vs. DAPA-control group; #$p < 0.05$ vs. diabetic group at 2 weeks.

(19). Eventually, left ventricular systolic function declines, leading to diabetic cardiomyopathy. Therefore, timely detection of early changes in cardiac structure and function in diabetic patients is of great clinical relevance (20). In this study, we built a diabetic model that was first fed a HFD for 8 weeks to induce insulin resistance and then injected with STZ to induce high glucose (21–23). Next, we performed comprehensive echo assessments at different time points in the process from prediabetes to earlyDM to evaluate the dynamic evolution of myocardial function and microvascular perfusion.
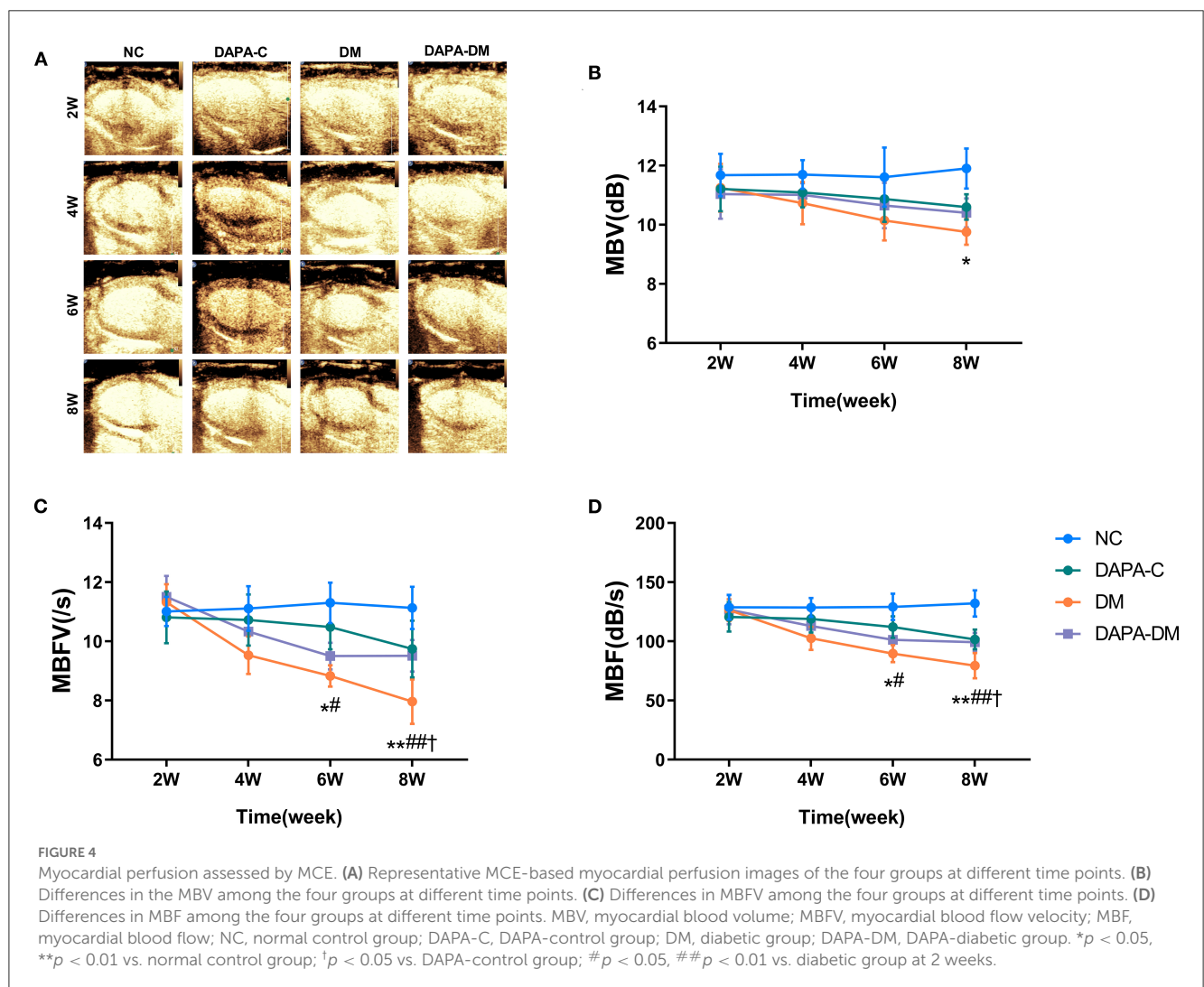
One major finding of this study is the advantage of 2D-STE and MCE, in comparison with conventional echo-Doppler techniques, for early detection of left ventricular deformity and abnormal microvascular and myocardial perfusion in prediabetes and earlyDM. In fact, no significant changes in left ventricular geometry or systolic and diastolic function were observed using conventional echo-Doppler parameters in diabetic rats, which is consistent with previous studies (24). Although tissue Doppler imaging has been utilized to evaluate myocardial motion, especially

when its direction is parallel to sound velocity, the accuracy of such measurements is angle dependent, limiting its value in assessing cardiac function in patients with diabetes (25). 2D-STE regards the myocardium as uniformly distributed acoustic spots and then tracks each spot and calculates its motion trajectory to accurately determine myocardial strain and strain rate (3). Previous studies have shown that 2D-STE can effectively reveal minor myocardial damage and provide quantitative assessment of left ventricular function in coronary heart disease (26), diabetic cardiomyopathy (27), and structural heart disease (28). Importantly, GLS is helpful in the early detection of subclinical myocardial dysfunction with preserved left ventricular EF for diabetic patients (27, 29). Likewise, MCE is adopted to dynamically evaluate the functional changes in myocardial microcirculation. Signal intensity in MCE imaging (microbubble volume) is thought to be equivalent to corresponding myocardial blood flow and has been used to estimate the local status of myocardial perfusion. Additionally, MCE has excellent temporal and spatial resolution and is low cost and simple to operate. Numerous experiments have shown that MCE is an effective

TABLE 3 Changes in myocardial perfusion parameters by MCE.

		Normal control ($n = 32$)	DAPA-control ($n = 32$)	Diabetic ($n = 32$)	DAPA-diabetic ($n = 32$)
2W	MBV (dB)	11.82 ± 1.94	10.94 ± 1.70	11.01 ± 2.33	10.75 ± 2.33
	MBFV (/s)	10.83 ± 1.17	10.91 ± 2.89	11.35 ± 1.96	11.08 ± 2.41
	MBF (dB/s)	128.59 ± 29.50	118.82 ± 35.95	123.04 ± 22.59	119.27 ± 38.62
4W	MBV (dB)	11.70 ± 1.37	11.19 ± 1.65	10.23 ± 1.08	11.09 ± 1.06
	MBFV (/s)	11.11 ± 2.14	10.99 ± 2.40	10.01 ± 1.98	10.39 ± 2.46
	MBF (dB/s)	128.58 ± 22.43	124.48 ± 39.40	103.41 ± 27.44	114.45 ± 26.18
6W	MBV (dB)	11.63 ± 2.82	11.33 ± 1.60	10.13 ± 1.88	10.66 ± 2.16
	MBFV (/s)	11.27 ± 1.94	10.42 ± 2.64	8.70 ± 0.83*#	9.44 ± 1.20
	MBF (dB/s)	129.03 ± 31.38	116.91 ± 28.46	88.04 ± 18.39*#	100.85 ± 25.51
8W	MBV (dB)	11.90 ± 1.91	11.11 ± 1.42	9.51 ± 1.53*	10.58 ± 1.43
	MBFV (/s)	10.99 ± 2.05	10.57 ± 1.58	7.86 ± 1.51***##†	9.58 ± 1.68
	MBF (dB/s)	130.96 ± 33.11	117.41 ± 24.84	74.85 ± 19.22***##†	102.13 ± 24.28

MBV, myocardial blood volume; MBFV, myocardial blood flow velocity; MBF, myocardial blood flow. *$p < 0.05$, **$p < 0.01$ vs. normal control group; †$p < 0.05$ vs. DAPA-control group; #$p < 0.05$, ##$p < 0.01$ vs. diabetic group at 2 weeks.

FIGURE 4
Myocardial perfusion assessed by MCE. **(A)** Representative MCE-based myocardial perfusion images of the four groups at different time points. **(B)** Differences in the MBV among the four groups at different time points. **(C)** Differences in MBFV among the four groups at different time points. **(D)** Differences in MBF among the four groups at different time points. MBV, myocardial blood volume; MBFV, myocardial blood flow velocity; MBF, myocardial blood flow; NC, normal control group; DAPA-C, DAPA-control group; DM, diabetic group; DAPA-DM, DAPA-diabetic group. *$p < 0.05$, **$p < 0.01$ vs. normal control group; †$p < 0.05$ vs. DAPA-control group; #$p < 0.05$, ##$p < 0.01$ vs. diabetic group at 2 weeks.
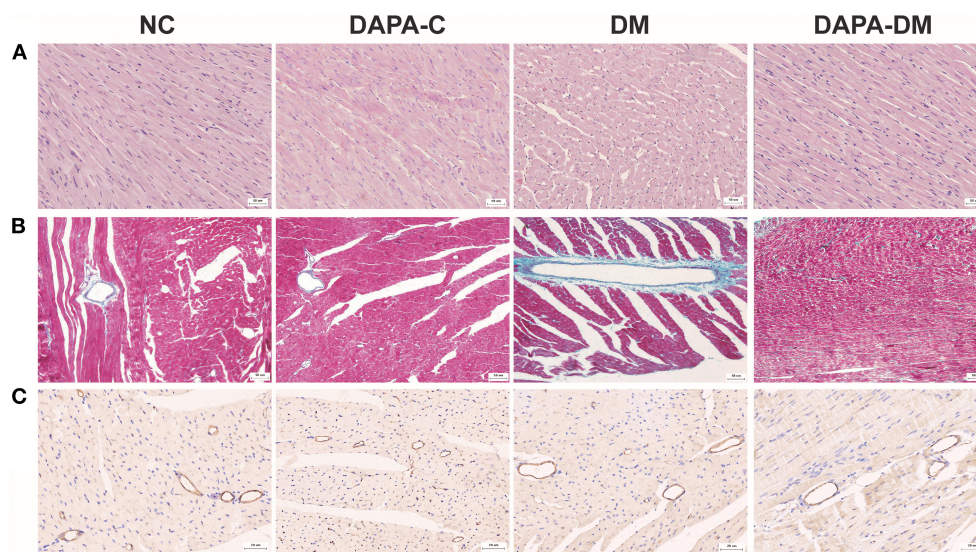
FIGURE 5
Typical pathological images of the four groups at 8 weeks. **(A)** Representative H&E staining images of the four groups at 8 weeks. Magnification: ×
200. **(B)** Representative Masson's trichrome staining images of the four groups at 8 weeks. Magnification: × 200. **(C)** Representative CD31 staining
images of the four groups at 8 weeks. Magnification: × 400. NC, normal control group; DAPA-C, DAPA-control group; DM, diabetic group;
DAPA-DM, DAPA-diabetic group.

method for detecting abnormal myocardial blood flow perfusion
(4) and that it is superior to positron emission tomography (PET)
and single photon emission computed tomography (SPECT) (30).

Another important finding is that DAPA exerts a beneficial
effect on left ventricular function and myocardial perfusion in
diabetic rats. SGLT2 inhibitors are a new class of oral hypoglycemic
drugs that can lower blood glucose levels by inhibiting sodium-
glucose reabsorption in proximal renal tubules and by promoting
urine glucose excretion. These agents not only effectively reduce
glycosylated hemoglobin but also have a low risk of hypoglycemia.
Recent studies have confirmed that DAPA slightly decreases
systolic and diastolic blood pressure, improves myocardial energy
utilization, and inhibits myocardial fibrosis. Recently, DAPA has
been embraced as a drug of choice for the treatment of heart
failure with reduced or preserved EF in diabetic and non-
diabetic patients (5, 10). In view of the significant advantages of
DAPA for cardiovascular benefits, we intended to apply DAPA in
prediabetes and earlyDM to explore its role in reversing myocardial
dysfunction by improving myocardial strain and microcirculation
in a rat model. Our results of 2D-STE and MCE studies
showed that indexes of left ventricular deformity (GLS, GCS,
and GRS) and parameters of myocardial perfusion (MBFV, MBF,
and MBV) gradually recovered to baseline levels after treatment
with DAPA, suggesting that the SGLT2 inhibitor DAPA may have
cardioprotective effects in this diabetic setting.

In addition, our histopathological study demonstrated that
myocardial cells were vacuolated and disorganized in prediabetes
and earlyDM. Increased collagen fibers deposition and decreased
myocardial microvascular density were also seen, which is in
line with previous reports (31). Interestingly, after treatment with
DAPA, myocardial cells became essentially normal with closely
packed cells. Furthermore, myocardial fibrosis and myocardial

microvascular density decreased were not as obvious. These results
further proved the effect of cardiovascular protection caused
by DAPA.

In conclusion, the findings of this experimental study
support the view that the combined use of 2D-STE and
MCE is more sensitive than the conventional Doppler-echo
technique for detecting impaired myocardial function and
microvascular perfusion in prediabetes and earlyDM. DAPA exerts
a beneficial effect on protecting left ventricular function and
myocardial perfusion in diabetic rats. This information may
provide experimental basis for the pathophysiology of diabetic
cardiomyopathy and should be useful to physicians who are
involved in decision-making for diabetic patients.

This study is subject to several limitations. First, the
current study focused on the changes in left ventricular
strain and microvascular perfusion in prediabetes and the
early stage of diabetes mellitus and the effect of DAPA
but did not focus on the changes in the late stage and
the corresponding role of DAPA. Future studies on the
changes in the late stage of diabetes and the role of
DAPA will be carried out. Second, in the present study,
resting MCE was performed; however, in the future,
stress MCE may be used to further evaluate myocardial
microvascular perfusion.

Data availability statement

The original contributions presented in the study
are included in the article/Supplementary material,
further inquiries can be directed to the
corresponding authors.

Ethics statement

The animal study was reviewed and approved by Laboratory Animal Welfare and Ethics Committee of the Third Military Medical University.

Author contributions

JL, YW, YSha, and YShe participated in study design, data analysis and interpretation, and drafting the manuscript. JL, JZ, XL, and LT performed experiments. JL, HH, YD, YSha, and YShe revised the manuscript before final approval. All authors read and approved the final manuscript.

Funding

Conflict of interest

The authors declare that the research was conducted in the absence of any commercial or financial relationships that could be construed as a potential conflict of interest.

Publisher's note

All claims expressed in this article are solely those of the authors and do not necessarily represent those of their affiliated organizations, or those of the publisher, the editors and the reviewers. Any product that may be evaluated in this article, or claim that may be made by its manufacturer, is not guaranteed or endorsed by the publisher.

Supplementary material

The Supplementary Material for this article can be found online at: https://www.frontiersin.org/articles/10.3389/fcvm.2023.1109946/full#supplementary-material

References

1. Nakamura K, Miyoshi T, Yoshida M, Akagi S, Saito Y, Ejiri K, et al. Pathophysiology and treatment of diabetic cardiomyopathy and heart failure in patients with diabetes mellitus. *Int J Mol Sci.* (2022) 23:3587. doi: 10.3390/ijms23073587

2. Konst RE, Guzik TJ, Kaski JC, Maas A, Elias-Smale SE. The pathogenic role of coronary microvascular dysfunction in the setting of other cardiac or systemic conditions. *Cardiovasc Res.* (2020) 116:817–28. doi: 10.1093/cvr/cvaa009

3. Todo S, Tanaka H, Yamauchi Y, Yokota S, Mochizuki Y, Shiraki H, et al. Association of left ventricular longitudinal myocardial function with subclinical right ventricular dysfunction in type 2 diabetes mellitus. *Cardiovasc Diabetol.* (2021) 20:212. doi: 10.1186/s12933-021-01404-5

4. Zhan J, Zhong L, Wu J. Assessment, treatment for coronary microvascular dysfunction by contrast enhanced ultrasound. *Front Cardiovasc Med.* (2022) 9:899099. doi: 10.3389/fcvm.2022.899099

5. Jhund PS, Kondo T, Butt JH, Docherty KF, Claggett BL, Desai AS, et al. Dapagliflozin across the range of ejection fraction in patients with heart failure: a patient-level, pooled meta-analysis of DAPA-HF, DELIVER. *Nat Med.* (2022) 28:1956–64. doi: 10.1038/s41591-022-01971-4

6. Cunningham JW, Vaduganathan M, Claggett BL, Kulac IJ, Desai AS, Jhund PS, et al. Dapagliflozin in patients recently hospitalized with heart failure, mildly reduced or preserved ejection fraction. *J Am Coll Cardiol.* (2022) 80:1302–10. doi: 10.1016/j.jacc.2022.07.021

7. Zhu Y, Zhang JL, Yan XJ, Sun L, Ji Y, Wang FF, et al. Effect of dapagliflozin on the prognosis of patients with acute myocardial infarction undergoing percutaneous coronary intervention. *Cardiovasc Diabetol.* (2022) 21:186. doi: 10.1186/s12933-022-01627-0

8. McMurray JJV, Solomon SD, Inzucchi SE, Køber L, Kosiborod MN, Martinez FA, et al. Dapagliflozin in patients with heart failure and reduced ejection fraction. *N Engl J Med.* (2019) 381:1995–2008. doi: 10.1056/NEJMoa1911303

9. Petrie MC, Verma S, Docherty KF, Inzucchi SE, Anand I, Belohlávek J, et al. Effect of Dapagliflozin on Worsening Heart Failure, Cardiovascular Death in Patients With Heart Failure With, Without Diabetes. *Jama.* (2020) 323:1353–68. doi: 10.1001/jama.2020.1906

10. Solomon SD, McMurray JJ, Claggett B, de Boer RA, DeMets D, Hernandez AF, et al. Dapagliflozin in heart failure with mildly reduced or preserved ejection fraction. *N Engl J Med*, (2022) 387:1089–1098. doi: 10.1056/NEJMoa2206286

11. Tei C, Ling LH, Hodge DO, Bailey KR, Oh JK, Rodeheffer RJ, et al. New index of combined systolic and diastolic myocardial performance: a simple, reproducible measure of cardiac function–a study in normal and dilated cardiomyopathy. *J Cardiol.* (1995) 26:357–66. doi: 10.1016/S0894-7317(05)80111-7

12. Cosyns B, Droogmans S, Hernot S, Degaillier C, Garbar C, Weytjens C, et al. Effect of streptozotocin-induced diabetes on myocardial blood flow reserve assessed by myocardial contrast echocardiography in rats. *Cardiovasc Diabetol.* (2008) 7:26. doi: 10.1186/1475-2840-7-26

13. Taqui S, Ferencik M, Davidson BP, Belcik JT, Moccetti F, Layoun M, et al. Coronary microvascular dysfunction by myocardial contrast echocardiography in nonelderly patients referred for computed tomographic coronary angiography. *J Am Soc Echocardiogr.* (2019) 32:817–25. doi: 10.1016/j.echo.2019.03.001

14. Vink CEM, van de Hoef TP, Götte MJW, Eringa EC, Appelman Y. Reduced microvascular blood volume as a driver of coronary microvascular disease in patients with non-obstructive coronary artery disease: rationale and design of the Micordis study. *Front Cardiovasc Med.* (2021) 8:730810. doi: 10.3389/fcvm.2021.730810

15. Boudina S, Abel ED. Diabetic cardiomyopathy revisited. *Circulation.* (2007) 115:3213–23. doi: 10.1161/CIRCULATIONAHA.106.679597

16. Aneja A, Tang WH, Bansilal S, Garcia MJ, Farkouh ME. Diabetic cardiomyopathy: insights into pathogenesis, diagnostic challenges, and therapeutic options. *Am J Med.* (2008) 121:748–57. doi: 10.1016/j.amjmed.2008.03.046

17. Wang M, Li Y, Li S, Lv J. Endothelial Dysfunction and Diabetic Cardiomyopathy. *Front Endocrinol (Lausanne).* (2022) 13:851941. doi: 10.3389/fendo.2022.851941

18. Muñoz-Córdova F, Hernández-Fuentes C, Lopez-Crisosto C, Troncoso MF, Calle X, Guerrero-Moncayo A, et al. Novel insights into the pathogenesis of diabetic cardiomyopathy, pharmacological strategies. *Front Cardiovasc Med.* (2021) 8:707336. doi: 10.3389/fcvm.2021.707336

19. Mohan M, Dihoum A, Mordi IR, Choy AM, Rena G, Lang CC, et al. Left ventricular hypertrophy in diabetic cardiomyopathy: a target for intervention. *Front Cardiovasc Med.* (2021) 8:746382. doi: 10.3389/fcvm.2021.746382

20. Marwick TH, Ritchie R, Shaw JE, Kaye D. Implications of underlying mechanisms for the recognition, management of diabetic cardiomyopathy. *J Am Coll Cardiol.* (2018) 71:339–51. doi: 10.1016/j.jacc.2017.11.019

21. Sadana P, Edler M, Aghayev M, Arias-Alvarado A, Cohn E, Ilchenko S, et al. (2022). Metabolic labeling unveils alterations in the turnover of HDL-associated proteins during diabetes progression in mice. *Am J Physiol Endocrinol Metab.* 323:E480–91. doi: 10.1152/ajpendo.00158.2022

22. Zhang L, Huang YJ, Sun JP, Zhang TY, Liu TL, Ke B, et al. Protective effects of calorie restriction on insulin resistance, islet function in STZ-induced type 2 diabetes rats. *Nutr Metab (Lond).* (2021) 18:48. doi: 10.1186/s12986-021-00575-y

23. Abdulmalek S, Eldala A, Awad D, Balbaa M. Ameliorative effect of curcumin, zinc oxide nanoparticles on multiple mechanisms in obese rats with induced type 2 diabetes. *Sci Rep.* (2021) 11:20677. doi: 10.1038/s41598-021-00108-w

24. Wang Y, Marwick TH. Update on echocardiographic assessment in diabetes mellitus. *Curr Cardiol Rep.* (2016) 18:85. doi: 10.1007/s11886-016-0759-0

25. Moudgil R, Hassan S, Palaskas N, Lopez-Mattei J, Banchs J, Yusuf SW, et al. Evolution of echocardiography in subclinical detection of cancer therapy-related cardiac dysfunction. *Echocardiography.* (2018) 35:860–8. doi: 10.1111/echo.14012

26. Xing X, Li D, Chen S, Wang L, Li Z, He L, et al. Evaluation of left ventricular systolic function in patients with different types of ischemic heart disease by two-dimensional speckle tracking imaging. *J Cardiothorac Surg.* (2020) 15:325. doi: 10.1186/s13019-020-01345-2

27. Minciună IA, Hilda Orăşan O, Minciună I, Lazar AL, Sitar-Tăut AV, Oltean M, et al. Assessment of subclinical diabetic cardiomyopathy by speckle-tracking imaging. *Eur J Clin Invest.* (2021) 51:e13475. doi: 10.1111/eci.13475

28. Huang X, Yue Y, Wang Y, Deng Y, Liu L, Di Y, et al. Assessment of left ventricular systolic, diastolic abnormalities in patients with hypertrophic cardiomyopathy using real-time three-dimensional echocardiography, two-dimensional speckle tracking imaging. *Cardiovasc Ultrasound.* (2018) 16:23. doi: 10.1186/s12947-018-0142-y

29. Albenque G, Rusinaru D, Bellaiche M, Lena CDi, Gabrion P, Delpierre Q, et al. Resting left ventricular global longitudinal strain to identify silent myocardial ischemia in asymptomatic patients with diabetes mellitus. *J Am Soc Echocardiogr.* (2022) 35:258–66. doi: 10.1016/j.echo.2021.10.013

30. Verkaik M, van Poelgeest EM, Kwekkeboom RFJ, Ter Wee PM, van den Brom CE, Vervloet MG, et al. Myocardial contrast echocardiography in mice: technical and physiological aspects. *Am J Physiol Heart Circ Physiol.* (2018) 314:H381–H391. doi: 10.1152/ajpheart.0024 2.2017

31. Seferovic PM, Paulus WJ. Clinical diabetic cardiomyopathy: a two-faced disease with restrictive, dilated phenotypes. *Eur Heart J.* (2015) 36:1718–1727a. doi: 10.1093/eurheartj/ehv134